

Atomistic modeling of electron-phonon coupling and transport properties in *n*-type [110] silicon nanowires

Wenxing Zhang,^{1,2} Christophe Delerue,¹ Yann-Michel Niquet,³ Guy Allan,¹ and Enge Wang⁴¹*Department ISEN, IEMN, 41 boulevard Vauban, 59046 Lille Cedex, France*²*Beijing National Laboratory for Condensed Matter Physics, Institute of Physics, Chinese Academy of Sciences, Beijing 100190, China*³*INAC, SP2M/L_Sim, CEA-UJF, 38054 Grenoble Cedex 9, France*⁴*School of Physics, Peking University, Beijing 100871, China*

(Received 5 July 2010; revised manuscript received 26 August 2010; published 22 September 2010)

Using a $sp^3d^5s^*$ tight-binding model for electrons and a valence force-field model for phonons, we study the transport properties of [110]-oriented silicon nanowires including all electron-phonon interactions. Using a full resolution of the Boltzmann transport equation, the low-field mobility is calculated and its dependence on the temperature, density of electrons, and size of the nanowires is investigated. We predict that, as a result of strong quantum confinement, (1) electrons couple to a wide and complex distribution of phonon modes and (2) the mobility has a nonmonotonic variation with wire diameter and is strongly reduced with respect to the bulk.

DOI: [10.1103/PhysRevB.82.115319](https://doi.org/10.1103/PhysRevB.82.115319)

PACS number(s): 73.63.Nm, 73.21.Hb

I. INTRODUCTION

Silicon nanowires (SiNWs) have attracted much attention due to their potential applications in various fields.¹ They are building blocks for nanoscale electronics and they can be fabricated by top-down (lithography) or bottom-up approaches (chemical growth) with a very good control of composition, size, and shape. SiNWs with diameters below 5 nm can now be manufactured.^{2–4} Therefore, it becomes extremely important to understand the transport properties of small SiNWs in order to predict the performance of ultimate transistors,^{4–10} sensors,¹¹ and thermoelectric devices.^{12,13} Several theoretical works^{14–24} have thus addressed the mobility in cylindrical SiNWs, including the electron-phonon (e-p) interaction which strongly influences the transport properties at room temperature.

The main issues in this context are (i) to determine key quantities such as scattering rates, mean-free paths and mobilities and (ii) to assess whether the transport properties of SiNWs are better or worse than those of bulk silicon. So far, experimental studies on the transport properties of SiNWs have led to somehow contradictory conclusions.^{5,25} On the theoretical side, it is known that quantum confinement tends to reduce the number of accessible channels for scattering,²⁶ which might increase the mobility. But there is a growing consensus that the mobility is actually reduced by the enhancement of the e-p coupling matrix elements.^{14–20} These predictions are based on various approximations. The electronic structure of the SiNWs is often calculated using effective-mass theory, sometimes using more accurate tight-binding (TB) methods which naturally include multiband effects, intervalley couplings and nonparabolic dispersions. Concerning phonons, a large number of works considered coupling to bulk phonons but other studies came to the conclusion that it is important to use confined phonons because there is a drastic modification of the acoustic-phonon modes by the confinement. In most cases, phonons are calculated using continuous models.

All previous theoretical studies consider only the lowest acoustic modes and use them in the e-p (intravalley or inter-

valley) coupling Hamiltonian with bulk deformation potentials. It is likely that these approximations are not justified in small SiNWs since the confinement influences both electrons and phonons, and therefore modifies the e-p coupling, as shown recently in Ref. 23. It is also important to include the coupling to other (higher acoustic and optical) modes because the confinement tends to mix all bulk phonon modes together in a quite complex manner. It was shown, for example, that only modes near the upper and lower bounds of the spectrum are purely optical or purely acoustic, while the other modes are, in general, a superposition of both with a gradually changing character.²⁷ In addition, if the low-field mobility is mostly governed by the coupling to the low-energy modes, coupling to higher modes becomes more important for hot carriers.

Therefore an improved description of the scattering of electrons by phonons in SiNWs is highly desirable. In a recent work,²² the effect of the e-p coupling on the current in a nanoscale transistor has been calculated using a Green's-function formalism for the transport, a tight-binding approach for the electronic structure and an atomistic model for the phonons. However, only the diagonal terms of the e-p self-energy could be considered, which is difficult to justify as recognized by the authors. Interestingly, it was shown that e-p coupling strongly reduces the current in transistors compared the ballistic case.

In this paper, we report a theoretical study on the transport properties of electrons in [110]-oriented SiNWs. In contrast to previous works, we have developed a fully atomistic approach for both electrons and phonons, and we have considered all the matrix elements of the e-p coupling Hamiltonian. We have used a combination of a TB method for the electronic structure and of a valence force-field method for the phononic structure. With this approach, we are able to calculate the scattering rates of electrons coupled to all phonon modes as a function of their energy. We show that a large distribution of modes is involved in the scattering. We compute the mobility in [110] wires and we show that it is strongly reduced with respect to the bulk situation due to an enhanced e-p coupling. We support the conclusion that the

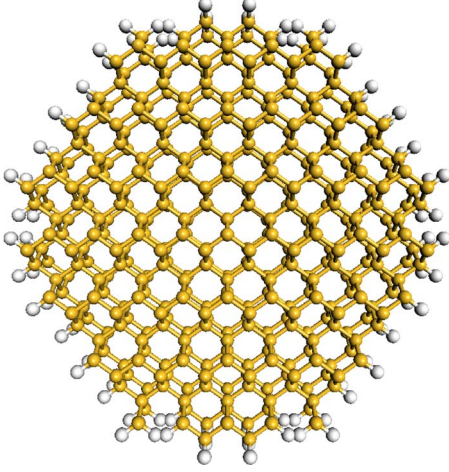


FIG. 1. (Color online) Structure of a 3.7 nm diameter [110] SiNW.

potential benefit of a lower density of states is counterbalanced by a higher e-p coupling strength leading in fact to a degraded mobility. We also demonstrate that atomistic modeling is required to study e-p coupling in small nanowires. By comparison with a recent theoretical work on the effects of surface roughness in SiNWs,²¹ we conclude that the e-p coupling remains the main limiting factor of the mobility at room temperature, at least in the configuration of disorder considered in that work. Our study combined with previous one (Ref. 21) demonstrates the possibility to study all the aspects of electron transport in nanostructures using atomistic approaches.

II. METHODOLOGY

We consider in the following free-standing undoped [110] SiNWs. We cut a cylinder from bulk Si and we saturate the dangling bonds with H atoms. The diameter of a SiNW is defined as²⁸ $d = \sqrt{Na^3/(2\pi l)}$, where a (5.431 Å) is the lattice constant of Si, N is the number of silicon atoms in the unit cell, and $l = a/\sqrt{2}$ is the length of the unit cell. Figure 1 illustrates the atomic structure of a 3.7 nm diameter [110] SiNW.

A. Electronic structure

The first nearest-neighbor $sp^3d^5s^*$ model is one of the most accurate and efficient TB descriptions of semiconductor materials. Usually, in TB, the effects of strains and atomic displacements are accounted for through the bond-length dependence of the nearest-neighbor parameters. However, Ref. 29 has shown recently that a much better description of the deformation potentials can be achieved with the introduction of strain-dependent on-site parameters in the $sp^3d^5s^*$ TB model. We have therefore used this model for the calculation of the electronic band structure and e-p coupling. It is important to note that the effects of arbitrary strains on the band energies and effective masses are reproduced in the full Brillouin zone, which is required to ensure a good transferability of the TB parameters from bulk to nanostructures.

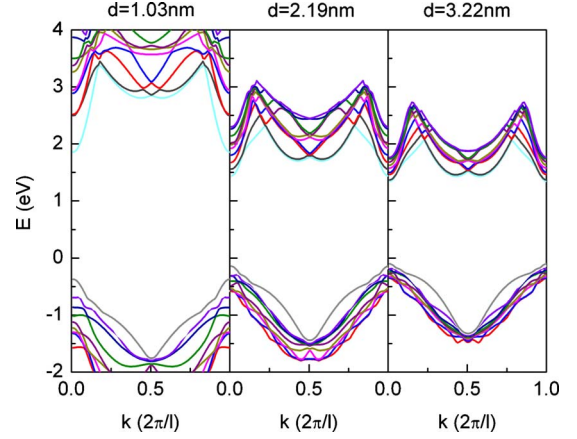


FIG. 2. (Color online) Electronic band structure of three [110] SiNWs with different diameters (for clarity, only 20 bands are plotted).

The electronic structure of [110] SiNWs is shown in Fig. 2. Two of the six bulk conduction-band (CB) minima project onto $k=0$ which is the actual conduction-band minimum of the nanowire²⁸ while the four others fold onto $k \approx \pm 0.8\pi/l$. The splitting between the two valleys (Fig. 4 of Ref. 28) strongly depends on size. The electrons around $k=0$ exhibit a lighter effective mass ($m^* \approx m_t = 0.19m_0$) along the nanowire than the electrons around $k \approx \pm 0.8\pi/l$ ($m^* \approx 0.55m_0$).

B. Phonon band structure

To describe the phonons, we have used the generalized Keating model proposed by Vanderbilt *et al.*³⁰ It reproduces accurately both the harmonic and anharmonic elastic properties of silicon, and provides a very good fit to the bulk phonon-dispersion curves. The elastic energy of the system is

$$\sum_i \frac{k_{rr}}{2} h_{ii}^2 + \sum_{i<j} \left[\frac{k_{\theta\theta}}{2} h_{ij}^2 + k_{r\theta}(h_{ii} + h_{jj})h_{ij} + k_{rr'}h_{ii}h_{jj} \right] + \sum_{i<j<k} k_{\theta\theta'}(h_{ij}h_{ik} + h_{ij}h_{jk} + h_{ik}h_{jk}) + \sum_{i<j<k} k_{\theta\theta''}h_{ij}h_{ik}, \quad (1)$$

where $h_{ii} = 16x_i^2/a^2 - 3$ and $h_{ij} = 16(\mathbf{x}_i \cdot \mathbf{x}_j + x_i^2/6 + x_j^2/6)/a$. Here i and j label nearest-neighbor bonds, and \mathbf{x}_i is the bond vector pointing from one atom to its neighbor. The coefficients $k_{\theta\theta}$, $k_{r\theta}$, $k_{rr'}$, $k_{\theta\theta'}$, and $k_{\theta\theta''}$ in Eq. (1) are given in Ref. 30 for Si-Si bonds. In the case of Si-H bonds at the surface, we have adjusted the parameters to reproduce the experimental bond-stretching and bond-angle vibration frequencies of SiH_4 and Si_2H_6 . We obtain $k_{rr'}^{\text{Si-H}} = 2.464$ eV, $k_{\theta\theta}^{\text{Si-H}} = 0.205$ eV, $k_{\theta\theta}^{\text{H-Si-H}} = 0.274$ eV, all other parameters being zero. The phonon band structure is computed from the dynamical matrices deriving from Eq. (1).

For SiNWs, there are four modes whose energies go to zero at the Γ point ($q=0$), as shown in Fig. 3. Two of these branches are linear in q and can be identified as the longitudinal- and transverse-acoustic phonons. The transverse phonon is actually a torsional mode of the wire. Furthermore, two other branches proportional to q^2 can be observed. They correspond to bending modes and are typical of

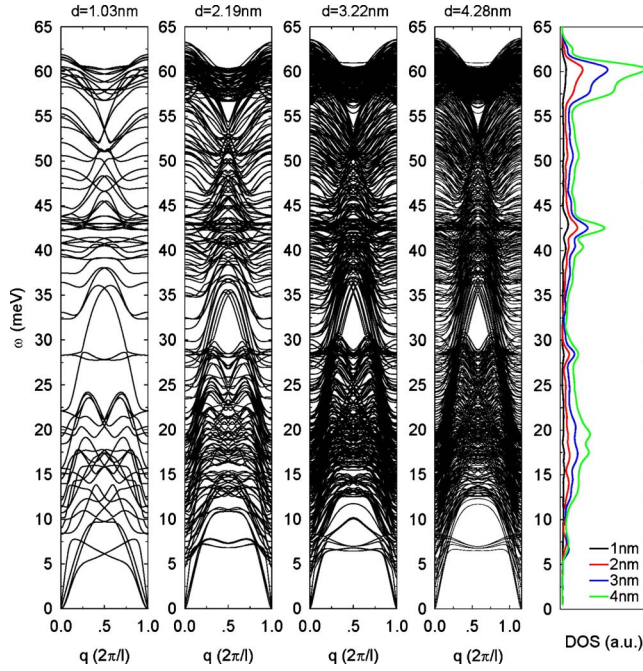


FIG. 3. (Color online) Phononic band structure of four [110] SiNWs with different diameters. The DOS for these nanowires is plotted in the right panel.

wires. Thonhauser *et al.*²⁷ and Peelaers *et al.*³¹ studied the phononic structure of [111] and [110] SiNWs and found the same behavior. The density of phonon states (DOS) computed from these band structures is plotted in the right panel of Fig. 3 while the corresponding transverse and longitudinal sound velocities are plotted as functions of the diameter in Fig. 4. Our values for small SiNWs agree well with *ab initio* calculations³¹ and rapidly tend to the bulk velocities at larger diameters.

C. Scattering rates

Using a first-order expansion of the Hamiltonian ($H = H^{(0)} + H^{(1)} + \dots$) as a function of the atomic displacements off equilibrium, we obtain the following formula for the e-p scattering matrix elements:

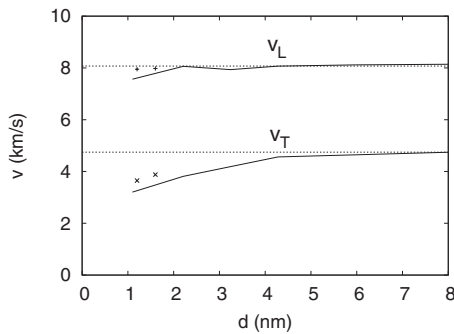


FIG. 4. Transversal (v_T) and longitudinal (v_L) acoustic sound velocities as functions of the diameter for [110] SiNWs. The horizontal lines are the bulk velocities. The *ab initio* values of Ref. 31 are given by symbols.

$$\begin{aligned} & \langle k+q, b' | \langle -q, j | H^{(1)} | 0 \rangle | k, b \rangle \\ & = \sum_{\alpha, i} \sqrt{\frac{\hbar}{2NM_\alpha \omega_j(q)}} e_{\alpha i}^{(j)}(q) \\ & \times \sum_{\beta \eta, \beta' \eta'} C_{\beta' \eta'}^{k+q, b'^*} C_{\beta \eta}^{k, b} \sum_{m, m'} e^{i\mathbf{k} \cdot \mathbf{R}_{m\beta}} e^{-i(\mathbf{k}+\mathbf{q}) \cdot \mathbf{R}_{m'\beta'}} \\ & \times \frac{\partial \langle \phi_{\eta'}(\mathbf{r} - \mathbf{R}_{m'\beta'}) | H | \phi_{\eta}(\mathbf{r} - \mathbf{R}_{m\beta}) \rangle}{\partial R_{0\alpha i}}. \end{aligned} \quad (2)$$

Equation (2) is the matrix element for the transition of an electron from the initial state $|k, b\rangle$ to the final state $|k+q, b'\rangle$ after emission of a phonon $| -q, j \rangle$ (same formula for absorption). k and q are the wave vectors of the electron and phonon, respectively, while b and j are the indexes of the electron band and phonon mode. $C_{\beta \eta}^{k, b}$ is an eigenvector element of $H^{(0)}$ at equilibrium, where β (α) is the atom index in the unit cell and η denotes the orbital type ($s, p_x, d_{x^2-y^2}, \dots$). $\phi_{\eta}(\mathbf{r} - \mathbf{R}_{m\beta})$ is the atomic orbital η centered on atom $\mathbf{R}_{m\beta}$ in the unit cell m . $e_{\alpha i}^{(j)}(q)$ is an eigenvector element of phonon state $|q, j\rangle$ and $\omega_j(q)$ is the corresponding eigenfrequency. $R_{0\alpha i}$ is the i component (x, y, z) of vector $\mathbf{R}_{0\alpha}$, N is the number of Wigner-Seitz unit cells, and M_α is the mass of atom α . The transition rate from a state $|k, b\rangle$ of energy $E_b(k)$ to a state $|k'=k+q, b'\rangle$ is given by Fermi's golden rule,

$$\begin{aligned} W_{kb, k'b'} = W(|k, b\rangle \rightarrow |k', b'\rangle) & = \frac{2\pi}{\hbar} \sum_j |\langle k', b' | \langle -q, j | H^{(1)} | 0 \rangle \\ & \times |k, b\rangle|^2 \times \{n(q, j) \delta[E_{k', b'} - E_{k, b} - \hbar \omega_j(q)] \\ & + [n(q, j) + 1] \delta[E_{k', b'} - E_{k, b} + \hbar \omega_j(q)]\}, \end{aligned} \quad (3)$$

where $n(q, j)$ is the equilibrium phonon occupation number (Bose-Einstein distribution).

D. Mobility

The low-field mobility μ is obtained by the resolution of the Boltzmann transport equation in the stationary regime. Under the application of a constant electric field F , the distribution function in the state $|k, b\rangle$ is given to the first-order in F by $f_b(k) = f^0(E_{k, b}) + eFg_b(k)$, where f^0 is the Fermi-Dirac distribution function and $g_b(k)$ is solution of the following equations:

$$\begin{aligned} & \sum_{b'} \int g_b(k) \{W_{kb, k'b'} [1 - f^0(E_{k', b'})] + W_{k'b', kb} f^0(E_{k', b'})\} \\ & - g_{b'}(k') \{W_{k'b', kb} [1 - f^0(E_{k, b})] + W_{kb, k'b'} f^0(E_{k, b})\} dk' \\ & = \frac{2\pi}{L} v_b(k) \left(\frac{\partial f^0}{\partial E} \right)_{E_{k, b}}, \end{aligned} \quad (4)$$

where $v_b(k) = \hbar^{-1} \partial E_{k, b} / \partial k$ is the group velocity and L is the length of the wire. The mobility is then given by

$$\mu = -e \frac{\sum_b \int g_b(k) v_b(k) dk}{\sum_b \int f^0(E_{k,b}) dk}. \quad (5)$$

E. Computational details

Injecting Eq. (3) into Eq. (4), we are left with terms of the form

$$\sum_{b'} \int u_{b',j}(q) \delta[E_{k',b'} - E_{k,b} \pm \hbar\omega_j(q)] dq, \quad (6)$$

where $u(q)$ is some function of q and $k' = k + q$. The evaluation of Eq. (6) is difficult due to the presence of the delta functions. The usual procedure is to replace each delta function by a Gaussian but we have found that the convergence of the calculations is slow. Therefore, we have used a numerically simpler but nevertheless more efficient method, valid in one dimension, taking advantage of the following property of the delta function:

$$\int_a^b F(x) \delta[G(x)] dx = \sum_i \frac{F(x_i)}{|G'(x_i)|}, \quad (7)$$

where the x_i are the solutions of $G(x) = 0$ in the interval $[a, b]$ and G' is the derivative of G . Equation (6) then becomes

$$\sum_{q,b',j} \left| \frac{u_{b',j}(q)}{\frac{\partial}{\partial q}[E_{k',b'} - E_{k,b} \pm \hbar\omega_j(q)]} \right|, \quad (8)$$

where the sum is restricted to the values of q , b' , and j that fulfill $E_{k',b'} - E_{k,b} \pm \hbar\omega_j(q) = 0$.

Practically, we specify a grid of k points in the first Brillouin zone and we consider a finite number of bands b that can be populated by electrons. The quantities $g_b(k)$ are the solutions of the linear system of Eq. (4), which are easily solved numerically. We calculate the phonon modes on a regular grid of q points. For each set of values of k and b , we determine all the solutions of $E_{k',b'} - E_{k,b} \pm \hbar\omega_j(q) = 0$ using a linear interpolation between successive q points. Typically, 300 k points are sufficient to converge the mobility and 1000 q points are required for a good interpolation. The calculation of the e-p coupling is thus very heavy. For example, in a SiNW with a diameter of 2.19 nm containing 72 Si and 28 H atoms per unit cell, there are 300 000 phonon modes if we include 1000 q points. Using ten conduction bands and 300 k points, the number of scattering processes that fulfill energy conservation is on the order of 10^6 . The calculation of the mobility for the largest nanowire considered in this work ($d = 3.7$ nm) required at total of $\sim 10^8$ s of CPU time, which was feasible thanks to an efficient parallelization of the code. We calculated the mobility on a cluster of 128 CPUs.

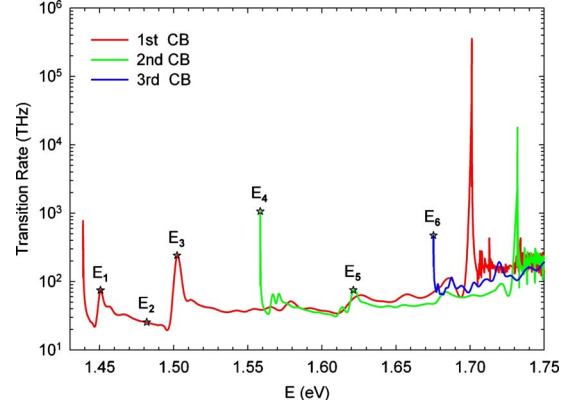


FIG. 5. (Color online) The total transition rate at room temperature ($T = 300$ K) versus electron energy in the lowest conduction bands of a 2.19 nm diameter [110] wire. First CB denotes the lowest-lying conduction band while second CB and third CB correspond to second and third conduction bands, respectively.

III. RESULTS AND DISCUSSION

A. Scattering rates

Figure 5 shows the total transition rate $\sum_{q,b'} W(|k, b\rangle \rightarrow |k + q, b'\rangle)$ of a specified initial electron state $|k, b\rangle$ versus the electron energy $E_{k,b}$ for a 2.19 nm diameter SiNW. Different peaks are clearly visible showing that, with increasing $E_{k,b}$, new channels fulfilling energy conservation are opened for scattering. We discuss the lowest CB (1CB) as an example (Fig. 5). At the 1CB edge (~ 1.44 eV), there is a marked peak due to intrasubband scattering by low-energy acoustic phonons. The second peak (E1) at ~ 1.45 eV is also due to scattering by low-energy acoustic modes. The peak (E3) at ~ 1.5 eV is mostly related to the intrasubband scattering by emission of high-energy acoustic phonons and optical phonons. There is another strong peak at ~ 1.7 eV which corresponds to the intrasubband scattering of electrons in the higher-energy valleys around $k \approx \pm 0.8\pi/l$. Obviously, these processes should only be important in hot-electron transport. The peaks at ~ 1.58 , ~ 1.63 , and ~ 1.66 eV in the 1CB contain an important contribution from intersubband scattering.

To clarify the contribution of the different phonon modes, we present in Fig. 6 the dependence of the transition rate on the phonon energy for specified electron states (labeled E1, E2, E3, E4, E5, and E6 in Fig. 5). A striking result of Fig. 6 is that there is a complex distribution of modes involved in the scattering and that this distribution strongly depends on the electron energy. This behavior is due to the strong quantum confinement which, to a large extent, breaks the selection rules that govern transitions in bulk Si. Figure 6 also shows that scattering by low-energy acoustic phonons does not remain the most efficient process at high enough energy above the conduction-band minima (see E3, E5).

We have found that the electrons do not couple to the modes localized at the surface and corresponding to Si-H vibrations. Even if we increase artificially the mass of the H atoms by a factor 5, the mobility remains basically unchanged. This is in agreement with the recent theoretical report that surface termination and chemistry have a rela-

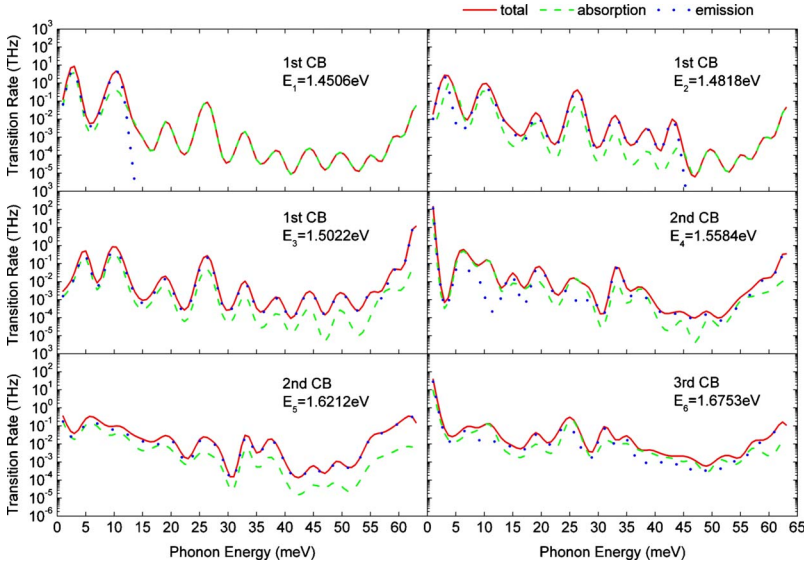


FIG. 6. (Color online) The transition rate ($T = 300$ K) as a function of the phonon energy for the electronic states E1, E2, E3, E4, E5, and E6 labeled in Fig. 5.

tively small influence on the phonon-limited mobility.²³

B. Mobility

Figure 7 shows the evolution of the low-field mobility as a function of the nanowire diameter. The mobility is calculated for two temperatures (77 and 300 K) and two electron densities ($n=10^{17}/\text{cm}^3$ and $n=10^{19}/\text{cm}^3$). The mobility strongly varies with size and tends to vanish as the diameter goes to zero. This confirms that, in spite of a reduced density of states, the mobility is decreased with respect to the bulk limit by the enhanced e-p coupling.^{14–20} In contrast to previous works, we also find that the mobility varies nonmonotonically with size. For example, the room-temperature mobility is smaller in 3.2 and 3.7 nm diameter SiNWs than in 2.7 nm diameter SiNWs. This is due to the increase in the population of electrons in the higher-lying subbands at $k=0$, and, at 300 K, to the increase in the population of the other valleys at $k \approx \pm 0.8\pi/l$, with larger effective masses and scattering rates. The effective mass in the lowest subband at $k=0$ is also slightly increasing with increasing diameter.²⁸

The nonmonotonic variations in the mobility are clearly visible at 77 K, where the Fermi-Dirac distribution function

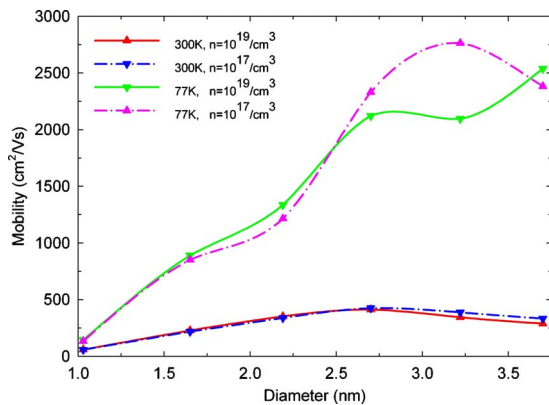


FIG. 7. (Color online) Mobility versus diameter for [110] SiNWs. Lines are only guide for the eyes.

is steeper around the Fermi energy. Only the two lowest-lying subbands at $k=0$ are occupied at 77 K but their respective populations strongly depend on size and carrier density. In 3.2 nm diameter SiNWs, the population of the second subband varies from 3 to 18% from $n=10^{17}$ to 10^{19} cm^{-3} while it weakly varies from 41 to 47% in 3.7 nm diameter SiNWs. Along with the rapid variations in the scattering rates with energy (Fig. 5), this explains the crossing of the mobility curves at 77 K.

We show in Table I the room-temperature population of electrons and mobility in the valleys at $k=0$ and $k \approx \pm 0.8\pi/l$. The splitting between these valleys decreases when the diameter of the nanowire increases.²⁸ The valleys at $k \approx \pm 0.8\pi/l$ therefore start to be populated for diameters >3 nm. The mobility is however smaller in these valleys due to the larger effective mass and stronger e-p coupling (Fig. 5), which decreases the average conductivity. Therefore the nonmonotonic variations in the mobility are direct consequences of quantum confinement, the mobility being determined by the number and population of channels open for scattering, by the complex distribution of phonon modes

TABLE I. Relative population p_v and mobility μ_v of the conduction-band valleys at $k=0$ and $k \approx \pm 0.8\pi/l$, at 300 K ($n = 10^{19} \text{ cm}^{-3}$). The mobility μ_v is defined by restricting the sum over bands in Eq. (5) to a given valley. The total mobility is, therefore, $\mu = \sum_v p_v \mu_v$.

Diameter (nm)	$k=0$		$k \approx \pm 0.8\pi/l$	
	Population (%)	Mobility ($\text{cm}^2/\text{V/s}$)	Population (%)	Mobility ($\text{cm}^2/\text{V/s}$)
1.0	100	60.0	0	
1.7	100	228.5	0	4.5
2.2	100	353.0	0	12.8
2.7	97	423.1	3	26.0
3.2	84	402.4	16	45.1
3.7	65	412.7	35	60.8

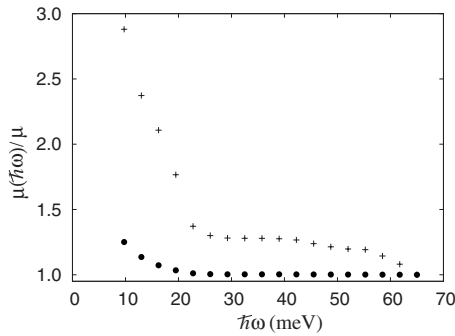


FIG. 8. Ratio $\mu(\hbar\omega)/\mu$ calculated at 300 K (+) and 77 K (●) for a 3.7 nm diameter SiNW ($n=10^{19}$ cm $^{-3}$). $\mu(\hbar\omega)$ is the mobility calculated taking into account only the phonons with energy below $\hbar\omega$ and μ is the total mobility including all the phonons [$\mu \equiv \mu(\hbar\omega > 65$ meV)].

coupling to the electrons, and by the e-p coupling matrix elements that depend on the electron energy. A good description of confined electron states, phonon modes, and e-p coupling is thus needed to predict accurately the transport properties of nanowires. For the small diameters considered here, this task clearly requires fully atomistic modeling. Note that we expect the mobility to increase again at larger diameters and to tend to the bulk value because the e-p coupling decreases.

Figure 8 illustrates which phonon modes influence the mobility in a 3.7 nm diameter SiNW. We plot $\mu(\hbar\omega)/\mu$, where $\mu(\hbar\omega)$ is the mobility calculated including only the scattering by phonons of energy below $\hbar\omega$. By definition, $\mu(\hbar\omega)=\mu$ for $\hbar\omega > 65$ meV when all the phonon modes are considered in the calculation of the mobility. At 77 K, only low-energy acoustic phonons contribute to inelastic scattering. But, at 300 K, we see that acoustic phonons with energy up to 25 meV are involved, and that there is also a small contribution from optical phonons above 45 meV.

In previous theoretical works on [110] nanowires, different values of the mobility were predicted although they were found in the same range as in Fig. 7. For example, at room temperature, a mobility of ~ 340 cm 2 /V/s was obtained in 4 nm diameter SiNWs by Ref. 17, and a mobility of ~ 800 cm 2 /V/s and ~ 500 cm 2 /V/s was predicted in 3.1 nm diameter SiNWs by Refs. 20 and 23, respectively. These results must be compared with our values of 388 cm 2 /V/s and 333 cm 2 /V/s for 3.2 nm and 3.7 nm diameter SiNWs, respectively (for $n=10^{17}$ cm $^{-3}$). Reference 20 used a $sp^3d^5s^*$ TB electronic structure quite similar to ours, as well as the same method to calculate the mobility. We conclude that their higher mobility is due to a simplified phonon band structure and e-p coupling Hamiltonian. Reference 23 used an *ab initio* approach to calculate the deformation potentials

but neglected higher subbands and employed an effective-mass approximation in the e-p coupling Hamiltonian and a simplified scheme to calculate the mobility, which explains the difference with our results.

Persson *et al.*²¹ have investigated the effect of surface roughness on charge transport in SiNWs. They used a sp^3 TB Hamiltonian which gives a similar band structure. They have considered a realistic surface roughness disorder and they have shown that the best orientation for electron transport without phonon scattering is the [110] direction with a mobility of 102, 315, and 1760 cm 2 /V/s for diameters of 1 nm, 2 nm, and 3 nm, respectively ($n=10^{18}$ cm $^{-3}$). Using a Green's-function approach, we have recently studied the influence of ionized P impurities on the mobility in [110] SiNWs surrounded by 2 nm of HfO $_2$ and a metallic gate.³² We obtain a room-temperature mobility of ~ 2730 cm 2 /V/s in 4 nm diameter SiNWs, for carrier and impurity concentrations $n=10^{18}$ cm $^{-3}$. Therefore, at room temperature, the e-p coupling is likely the dominant scattering mechanism for electrons in gate, all around SiNWs, for donor concentration below a few 10^{18} cm $^{-3}$. At low temperature, surface roughness or impurity scattering effects become more important.

IV. CONCLUSION

In conclusion, we have studied e-p coupling and the low field electron mobility in *n*-type [110] SiNWs, using a $sp^3d^5s^*$ TB model for the electronic structure and a valence force-field model for the phononic structure. All e-p scatterings are included in the calculation of the mobility. Our calculations have unveiled which phonon scatterings dominate electron transport properties in small SiNWs. For electrons close to the conduction-band minimum, almost all scatterings are intrasubband acoustic processes. For electrons with higher energy, intersubband scatterings and scatterings with other phonon modes become important. The effects of the quantum confinement on the electrons and the phonons have a large impact on the mobility which varies nonmonotonically with the SiNW diameter. Our work demonstrates that a fully atomistic approach is required for a proper description of e-p scattering in small nanostructures.

ACKNOWLEDGMENTS

Wenxing Zhang is grateful to the Co-tutorial-PhD project supported by French Embassy in China. This work was supported by the French National Research Agency (ANR) project QUANTAMONDE (Contract No. ANR-07-NANO-023-02) and by the Délégation Générale pour l'Armement, French Ministry of Defense under Grant No. 2008.34.0031. Part of the calculations were run at the CCRT supercomputing center.

- ¹*Nanosilicon*, edited by V. Kumar (Elsevier Science, Oxford, 2007).
- ²D. D. Ma, C. S. Lee, F. C. K. Au, S. Y. Tong, and S. T. Lee, *Science* **299**, 1874 (2003).
- ³Y. Wu, Y. Cui, L. Huynh, C. J. Barrelet, D. C. Bell, and C. M. Lieber, *Nano Lett.* **4**, 433 (2004).
- ⁴J. Goldberger, A. I. Hochbaum, R. Fan, and P. D. Yang, *Nano Lett.* **6**, 973 (2006).
- ⁵Y. Cui, Z. H. Zhong, D. L. Wang, W. U. Wang, and C. M. Lieber, *Nano Lett.* **3**, 149 (2003).
- ⁶C. Thelander, L. E. Fröberg, C. Rehnstedt, L. Samuelson, and L.-E. Wemersson, *IEEE Electron Device Lett.* **29**, 206 (2008).
- ⁷C. Dupré, T. Ernst, V. Maffim-Alvaro, V. Delaye, J. M. Hartmann, S. Borel, C. Vizoz, O. Faynot, G. Ghibaudo, and S. Deleonibus, *Solid-State Electron.* **52**, 519 (2008).
- ⁸V. Schmidt, H. Riel, S. Senz, S. Karg, W. Riess, and U. Gösele, *Small* **2**, 85 (2006).
- ⁹M. T. Björk, O. Hayden, H. Schmid, H. Riel, and W. Riess, *Appl. Phys. Lett.* **90**, 142110 (2007).
- ¹⁰M. Lundstrom and J. Guo, *Nanoscale Transistors: Device Physics, Modeling and Simulation* (Springer, New York, 2006).
- ¹¹Y. Cui, Q. Q. Wei, H. K. Park, and C. M. Lieber, *Science* **293**, 1289 (2001).
- ¹²A. I. Hochbaum, R. Chen, R. D. Delgado, W. Liang, E. C. Garnett, M. Najarian, A. Majumdar, and P. Yang, *Nature (London)* **451**, 163 (2008).
- ¹³T. Markussen, A.-P. Jauho, and M. Brandbyge, *Phys. Rev. Lett.* **103**, 055502 (2009).
- ¹⁴G. D. Sanders, C. J. Stanton, and Y. C. Chang, *Phys. Rev. B* **48**, 11067 (1993).
- ¹⁵J. Lee and M. O. Vassell, *J. Phys. C* **17**, 2525 (1984).
- ¹⁶R. Kotlyar, B. Obradovic, P. Matagne, M. Stettler, and M. D. Giles, *Appl. Phys. Lett.* **84**, 5270 (2004).
- ¹⁷E. B. Ramayya, D. Vasileska, S. M. Goodnick, and I. Knezevic, *IEEE Trans. Nanotechnol.* **6**, 113 (2007).
- ¹⁸E. B. Ramayya, D. Vasileska, S. M. Goodnick, and I. Knezevic, *J. Appl. Phys.* **104**, 063711 (2008).
- ¹⁹V. A. Fonoberov and A. A. Balandin, *Nano Lett.* **6**, 2442 (2006).
- ²⁰A. K. Buin, A. Verma, A. Svizhenko, and M. P. Anantram, *Nano Lett.* **8**, 760 (2008a).
- ²¹M. P. Persson, A. Lherbier, Y.-M. Niquet, F. Triozon, and S. Roche, *Nano Lett.* **8**, 4146 (2008).
- ²²M. Luisier and G. Klimeck, *Phys. Rev. B* **80**, 155430 (2009).
- ²³F. Murphy-Armando, G. Fagas, and J. C. Greer, *Nano Lett.* **10**, 869 (2010).
- ²⁴A. K. Buin, A. Verma, and M. P. Anantram, *J. Appl. Phys.* **104**, 053716 (2008b).
- ²⁵O. Gunawan, L. Sekaric, A. Majumdar, M. Rooks, J. Appenzeller, J. W. Sleight, S. Guha, and W. Haensch, *Nano Lett.* **8**, 1566 (2008).
- ²⁶H. Sakaki, *Jpn. J. Appl. Phys., Part 2* **19**, L735 (1980).
- ²⁷T. Thonhauser and G. D. Mahan, *Phys. Rev. B* **69**, 075213 (2004).
- ²⁸Y.-M. Niquet, A. Lherbier, N. H. Quang, M. V. Fernández-Serra, X. Blase, and C. Delerue, *Phys. Rev. B* **73**, 165319 (2006).
- ²⁹Y.-M. Niquet, D. Rideau, C. Tavernier, H. Jaouen, and X. Blase, *Phys. Rev. B* **79**, 245201 (2009).
- ³⁰D. Vanderbilt, S. H. Taole, and S. Narasimhan, *Phys. Rev. B*, **40**, 5657 (1989).
- ³¹H. Peelaers, B. Partoens, and F. M. Peeters, *Nano Lett.* **9**, 107 (2009).
- ³²M. P. Persson, H. Mera, Y.-M. Niquet, C. Delerue, and M. Diarra, *Phys. Rev. B* **82**, 115318 (2010).